IEEE Access
Multidisciplinary | Rapid Review | Open Access Journal

Received January 27, 2019, accepted February 23, 2019, date of publication March 8, 2019, date of current version April 1, 2019.

Digital Object Identifier 10.1109/ACCESS.2019.2903732

Generalized Real-Valued Weighted Covariance-Based Detection Methods for Cognitive Radio Networks With Correlated Multiple Antennas

AN-ZHI CHEN[1], ZHI-PING SHI[1], (Member, IEEE), AND JIAN XIONG[2], (Member, IEEE)
[1]National Key Laboratory of Science and Technology on Communications, University of Electronic Science and Technology of China, Chengdu 611731, China
[2]Department of Electronic Engineering, Shanghai Jiao Tong University, Shanghai 200240, China

Corresponding author: Zhi-Ping Shi (szp@uestc.edu.cn)

This work was supported by the Natural Science Foundation of China under Grant 61671128 and Grant 61671295.

ABSTRACT This paper is concerned with the spectrum sensing problem for cognitive radio networks with correlated receiving multiple antennas in the time-varying fading channel. We first consider the scenario that all the antennas have the same noise variance and present a generalized real-valued weighted-covariance-based detection (GRWCD) method. In particular, we derive the distribution of the GRWCD statistic under the null hypothesis, which allows us to develop the theoretical decision threshold for a given false alarm probability. Besides, we derive the distribution of the GRWCD statistic under the alternative hypothesis, which enables us to provide a mathematical expression for the detection probability as well as the theoretical receiver operating characteristic. Meanwhile, we consider a more general scenario of unequal per-antenna noise variances and present a modified GRWCD method as well as the theoretical expressions of the decision threshold. The simulation results are provided to verify the accuracy of the derived results and show that the proposed two methods are capable of providing performance improvement over several advanced methods in the literature.

INDEX TERMS Spectrum sensing, correlated receiving multiple antennas, time-varying fading channel, cognitive radio network.

I. INTRODUCTION

Cognitive radio (CR) based communication networks have been put forward as a promising paradigm for designing the upcoming fifth-generation wireless networks, due to its unprecedented advantage in spectral efficiency [1]–[4]. The key concept of CR is to allow unlicensed secondary users (SUs) to opportunistically access the licensed bands originally allocated to the licensed primary users (PUs), when no communication activity is needed for PUs. To use the licensed bands scrupulously without interfering the PUs, the SUs should firstly probe the activity states of PUs within a given sensing time through spectrum sensing (SS) procedure.

Nowadays, there have been many detection methods for spectrum sensing [5]–[7]. Traditional methods include energy detection (ED) [8]–[12], matched filter detection (MFD) [13]–[15] and cyclostationarity feature detection (CFD) [16]–[19]. Each method may be preferable compared with others, depending on the available resources, information and the environment conditions. For example, when the SU has prior information regarding the PU's signal characteristics, the MFD is considered to be an optimal coherent detection method for detecting the PU. However, obtaining prior information about the transmitted signal is unworkable in most practical applications. If there is a priori knowledge available regarding the cyclic frequency of the PU's signal, the CFD is a popular choice for SS. However, its performance heavily relies on the accurate knowledge of cyclic frequency, a small cyclic frequency offset can lead to significant performance degradation. Also, the CFD method suffers a high computational complexity, which hinders its application in real time detection. Unlike the above two detection methods, ED does not require any priori information about the PU's signal and moreover, it has the lowest computational complexity among these methods. Despite its advantages, howbeit ED requires the exact knowledge of noise variance to calculate the decision threshold.

The associate editor coordinating the review of this manuscript and approving it for publication was Xiaofei Wang.

Otherwise, it suffers from severe performance degradation in the presence of noise uncertainty due to the SNR wall phenomenon [20].

When multiple antennas are available at the SU, the detectors can overcome the aforementioned limitations, such as the maximum-minimum eigenvalue (MME) [21], covariance absolute value (CAV) [22], covariance Frobenius norm (CFN) [22], arithmetic-to-geometric mean (AGM) [23], scaled largest eigenvalue (SLE) [24], locally most powerful invariant test (LMPIT) [25], Hadamard ratio test [26], volume-based detection (VD) [27], [28] and eigenvalue moment ratio (EMR) [29] methods have been proposed without any prior knowledge and can deliver desirable performance. Whereas, these detection methods focused mainly on time-invariant channels (i.e., channel state remains unchanged during a sensing period), and may not perform well in time-varying channels. Stemming from this point, Jin *et al.* [30] studied the SS problem for CR network with correlated receiving multiple antennas in a time-varying fading channel, and based on the CAV method, a weighted-covariance-based detection (WCD) method was proposed in their work. Moreover, they showed that the WCD method can achieve significant performance improvements in comparison with the CAV and CFN methods. However, the WCD method involves huge complex computations. Furthermore, although an expression for the detection probability was presented in [30], but was not given in closed form. Toward this end, in our earlier work [31], we converted the complex-valued SS problem described by [30] into the real-valued SS problem and proposed a reduced-complexity real-valued WCD (RWCD) method. Moreover, we derived an asymptotic closed-form expression of the detection probability to gain further insights into the RWCD method and demonstrated that the RWCD method achieved almost the same performance as the original WCD method, but with a lower computational cost. However, the RWCD method is derived under the assumption of uniform noise variances across the antennas, in practice, such an assumption may not hold because the SU receivers are usually uncalibrated.

Motivated by the above researches, this paper focuses on the SS problem for CR networks with correlated receiving multiple antennas in time-varying fading channels. To sum up, the main contribution of this work is twofold.

1) We first consider the scenario where the noise at all antennas have the same variance, and develop a generalized RWCD (GRWCD) method for such a scenario. The distributions of the GRWCD statistic under the null and alternate hypotheses are first derived. With the derived distributions, we present the theoretical expressions of the decision threshold and detection probability for the proposed method, which can help bring insights to the theoretical findings. Also, we show that the RWCD method given in [31] can be regarded as a special case of our proposed one.
2) In particular, we consider the scenario that the noise variances at all antennas are non-uniform, which was not considered in our earlier work [31], and a modified GRWCD (MGRWCD) method is proposed.

Finally, experimental results reveal that the proposed two methods are capable of providing performance improvement over several advanced methods in the literature, including the RWCD method.

Notation: The operations $\sim$, $|\cdot|$, $(\cdot)^*$ and $(\cdot)^T$ indicate "distributed as", absolute value, conjugate operator and vector transpose, respectively. $\mathbb{E}[x]$ and $\mathbb{D}[x] = \mathbb{E}[x^2] - \mathbb{E}^2[x]$ represent the statistical expectation and variance of random variable x, respectively. $\mathcal{N}(\mu_r, \sigma^2)$ denotes the real Gaussian distribution with mean μ_r and covariance σ^2, $\mathcal{CN}(\mu_c, \Sigma)$ stands for the circularly symmetric complex Gaussian (CSCG) distribution with mean μ_c and covariance Σ. $\mathbf{I}_M$ and $\mathbf{0}_M$ are the $M \times M$ identity matrix and $M \times 1$ zero column vector, respectively. a_{mn} denotes the (m, n)th element of a matrix $\mathbf{A}$. The positive odd integer and nonnegative even integer are denoted by $\mathbf{O}_+$ and $\mathbf{E}_0$, respectively. $\Gamma(\cdot)$ and $\Phi(\cdot, \cdot; \cdot)$ are the gamma and Kummer's confluent hypergeometric functions [32], respectively. The real and imaginary parts of e are denoted by e^r and e^i, respectively. diag$\{\mathbf{x}\}$ denote the diagonal matrix with diagonal elements from vector $\mathbf{x}$.

II. SYSTEM MODEL

A. PROBLEM DESCRIPTION

We consider a CR network that consists of a one-antenna PU and an M-antenna SU operating over time-varying Rayleigh fading channels, in which SS is performed by the SU to identify the presence or absence of the PU's signal in a given spectrum band. Let denote the hypotheses of the idleness and activeness of the PU by $\mathcal{H}_0$ and $\mathcal{H}_1$, respectively. Assume that each antenna collects K samples within a sensing time, the received signal vector $\mathbf{r}(k) \in \mathbb{C}^{M\times 1}$ at the SU can then be expressed by

$$\begin{cases} \mathcal{H}_0: & \mathbf{r}(k) = \mathbf{w}(k), \\ \mathcal{H}_1: & \mathbf{r}(k) = \mathbf{h}(k)s(k) + \mathbf{w}(k), \end{cases} \quad k = 1, \ldots, K, \quad (1)$$

where k is the time index, $s(k) \sim \mathcal{CN}(0, \sigma_s^2)$ is the transmitted signal from the PU, and $\mathbf{h}(k) \sim \mathcal{CN}(\mathbf{0}_M, \sigma_h^2\mathbf{\Phi})$ denotes the Rayleigh fading channel vector from the PU to the SU, in which $\mathbf{\Phi}$ and σ_h^2 denote the receive-side correlation matrix and channel power, respectively. Additionally, $\mathbf{w}(k) \in \mathbb{C}^{M\times 1}$ is the additive CSCG noise vector with mean zero and unknown diagonal covariance matrix $\mathbf{R}_w = \text{diag}\{\sigma_{w1}^2, \sigma_{w2}^2, \ldots, \sigma_{wM}^2\}$. If $\mathbf{R}_w = \sigma_w^2\mathbf{I}_M$, the noise variances at all antennas are uniform, otherwise non-uniform. Without loss of generality, $s(k)$, $\mathbf{h}(k)$ and $\mathbf{w}(k)$ are assumed to be statistically independent of each other. The received signal-to-noise ratio (SNR) in power ratio is defined as $\frac{M\sigma_s^2\sigma_h^2}{\text{tr}(\mathbf{R}_w)}$, where tr$(\mathbf{R}_w)$ denote the trace of $\mathbf{R}_w$.

B. CHANNEL MODEL

In this work, we consider the spatial correlation between antenna elements at SU, and the exponential model is

adopted here to describe such spatial correlation. As a result, the (m, n)th element of the receive-side correlation matrix $\mathbf{\Phi}$ is given by [33]

$$\mathbf{\Phi}_{mn} = \begin{cases} \rho^{n-m}, & m \le n \\ \mathbf{\Phi}^*_{nm}, & m > n, \end{cases} \quad m, n = 1, \ldots, M, \tag{2}$$

where ρ $(0 \le \rho \le 1)$ is a real-valued correlation coefficient between two neighboring antennas. With this, the spatially correlated Rayleigh fading channel $\mathbf{h}(k)$ can be modeled as [31]

$$\mathbf{h}(k) = \mathbf{\Phi}^{1/2}\widetilde{\mathbf{h}}(k), \quad k = 1, \ldots, K, \tag{3}$$

where $\mathbf{\Phi}^{1/2}$ is the matrix square root of $\mathbf{\Phi}$, and $\widetilde{\boldsymbol{h}}(k) \sim \mathcal{CN}(\mathbf{0}_M, \mathbf{I}_M)$ is an independent and identically distributed (i.i.d.) CSCG random vector.

III. GENERALIZED REAL-VALUED WEIGHTED COVARIANCE-BASED DETECTOR

A. SUGGESTED METHOD I: GRWCD

The method presented in this subsection assume that the noises at all antennas have the same variance σ_w^2 (i.e., $\sigma_{w1}^2 = \sigma_{w2}^2 = \ldots = \sigma_{wM}^2 = \sigma_w^2$). In our previous work [31], the complex-valued SS problem described by (1) were converted into real-valued SS problem, as given by

$$\begin{cases} \mathcal{H}_0: & \begin{cases} \mathbf{r}^r(k) = \mathbf{w}^r(k), \\ \mathbf{r}^i(k) = \mathbf{w}^i(k); \end{cases} \\ \mathcal{H}_1: & \begin{cases} \mathbf{r}^r(k) = \mathbf{h}^r(k)s^r(k) - \mathbf{h}^i(k)s^i(k) + \mathbf{w}^r(k), \\ \mathbf{r}^i(k) = \mathbf{h}^r(k)s^i(k) + \mathbf{h}^i(k)s^r(k) + \mathbf{w}^i(k). \end{cases} \end{cases} \tag{4}$$

where $\mathbf{r}^r(k)$ and $\mathbf{r}^i(k)$ are the real and imaginary parts of the received signal vector $\mathbf{r}(k)$, respectively. Under $\mathcal{H}_0$, $\mathbf{r}^r(k)$ and $\mathbf{r}^i(k)$ are independent, both have zero mean and covariance matrix $(\sigma_w^2/2)\mathbf{I}_M$. While, under $\mathcal{H}_1$, $\mathbf{r}^r(k)$ and $\mathbf{r}^i(k)$ are uncorrelated, both have zero mean and covariance matrix $(\sigma_s^2\sigma_h^2/2)\mathbf{\Phi} + (\sigma_w^2/2)\mathbf{I}_M$. Notice form the above that the covariance matrices of $\mathbf{r}^r(k)$ and $\mathbf{r}^i(k)$ differ between the hypotheses $\mathcal{H}_0$ and $\mathcal{H}_1$, which can be used to detect the presence of PU's signals. To lay the groundwork for the proposed method, in the following, we will first recall the RWCD method [31] for the SS problem in (4).

In [31], the sample covariance matrix from the K received signal vectors is first computed, as given by

$$\hat{\mathbf{A}} = \frac{1}{2K}\sum_{k=1}^{K}\left[\mathbf{r}^r(k)\left(\mathbf{r}^r(k)\right)^T + \mathbf{r}^i(k)\left(\mathbf{r}^i(k)\right)^T\right]. \tag{5}$$

Then, the estimated power of the observed signal is computed as follows:

$$\hat{\sigma}_w^2 = \frac{1}{M}\sum_{m=n}\hat{a}_{mn}, \tag{6}$$

where $\hat{a}_{mn}$ is the (m, n)th element of $\hat{\mathbf{A}}$.

Later, the estimated elements $a'_{mn}(m < n)$ and weight coefficients $w_l(l = 1, \ldots, M-1)$ are computed as

$$a'_{mn} = \frac{\hat{a}_{mn}}{\hat{\sigma}_w^2}, \tag{7}$$

$$w_l = \sum_{n-m=l} a'_{mn}. \tag{8}$$

Finally, the test statistic and decision rule of the RWCD are given as follows:

$$T_R = \sum_{l=1}^{M-1}\left(w_l \sum_{n-m=l}|a'_{mn}|\right) \underset{H_0}{\overset{H_1}{\gtrless}} \lambda_R, \tag{9}$$

where λ_R is the decision threshold of the RWCD method.

By adding a power operation p $(0 < p \le 1)$ on $|a'_{mn}|$, we now propose a GRWCD method as follow:

$$T_G \triangleq \sum_{l=1}^{M-1}\left(w_l \sum_{n-m=l}|a'_{mn}|^p\right) \underset{\mathcal{H}_0}{\overset{\mathcal{H}_1}{\gtrless}} \lambda_G, \tag{10}$$

where T_G and λ_G are the test statistic and decision threshold of the proposed GRWCD method, respectively. Careful inspection of (15) reveals that the RWCD method in [31] can be viewed as a special case our proposed one when $p = 1$. Moreover, as we will shown in our simulations, the proposed GRWCD method is capable of outperforming the RWCD method.

B. SUGGESTED METHOD II: MGRWCD

It can be observed that, for the RWCD and GRWCD methods, the estimated elements a'_{mn} in (7) are based on the assumption that the noise variances at all antennas must be equal, otherwise, they cannot offer a high sensing performance. In this subsection, to relax such a assumption, we consider a more general scenario that the noises at different antennas have unequal variances (i.e., $\sigma_{w1}^2 \ne \sigma_{w2}^2 \ne \ldots \ne \sigma_{wM}^2$), and present an MGRWCD method here.

Step 1: The first step is the same as that in (5);

Step 2: Compute the square root of the estimated power $\hat{a}_{mm}$ at the mth antenna via

$$\hat{\sigma}_{wm} = \sqrt{\hat{a}_{mm}}, \quad m = 1, \ldots, M. \tag{11}$$

Step 3: Compute the estimated elements $c'_{mn}(m < n)$ via

$$c'_{mn} = \frac{\hat{a}_{mn}}{\hat{\sigma}_{wm}\hat{\sigma}_{wn}} \tag{12}$$

Step 4: Compute the weight coefficients $\tau_l(l = 1, \ldots, M-1)$ via

$$\tau_l = \sum_{n-m=l} c'_{mn} \tag{13}$$

Step 5: After the above four steps, the test statistic and decision rule of the MGRWCD method are given by

$$T_M \triangleq \sum_{l=1}^{M-1}\left(\tau_l \sum_{n-m=l}|c'_{mn}|\right) \underset{\mathcal{H}_0}{\overset{\mathcal{H}_1}{\gtrless}} \lambda_M, \tag{14}$$

where λ_M is the decision threshold of the MGRWCD method.

IV. PERFORMANCE ANALYSIS

For facilitating the development of the theoretical analysis, the following Proposition 1 is introduced.

Proposition 1: Suppose that $\eta \sim \mathcal{N}(\mu, \sigma^2)$ is a real Gaussian random variable with mean μ and variance σ^2. Then, for a nonnegative integer q and real number ξ $(0 < \xi \leq 1)$, the expectation of $\eta^q|\eta|^\xi$ is given as follow.

1): If $q \in \mathbf{O}_+$,

$$\mathbb{E}\left[\eta^q|\eta|^\xi\right] = \mu\sigma^{\xi+q-1}2^{\frac{1-\xi-q}{2}}e^{-\frac{\mu^2}{2\sigma^2}}\frac{\Gamma(\xi+q+1)}{\Gamma(\frac{\xi+q+1}{2})} \times \Phi\Big(\frac{\xi+q+2}{2}, \frac{3}{2}; \frac{\mu^2}{2\sigma^2}\Big).$$

2): If $q \in \mathbf{E}_0$,

$$\mathbb{E}\left[\eta^q|\eta|^\xi\right] = \sigma^{\xi+q}2^{\frac{\xi+q}{2}}\frac{\Gamma(\frac{\xi+q+1}{2})}{\sqrt{\pi}}\Phi\Big(-\frac{\xi+q}{2}, \frac{1}{2}; -\frac{\mu^2}{2\sigma^2}\Big).$$

Proof: Case 1: For a positive odd integer q, we have

$$\begin{aligned}\mathbb{E}\left[\eta^q|\eta|^\xi\right] &= \frac{1}{\sqrt{2\pi\sigma^2}}\int_{-\infty}^{\infty}\eta^q|\eta|^\xi e^{-\frac{(\eta-\mu)^2}{2\sigma^2}}d\eta \\ &= \frac{2^{\frac{\xi+q}{2}}\sigma^{\xi+q}}{\sqrt{\pi}}e^{-\frac{\mu^2}{2\sigma^2}}\Bigg[\underbrace{\int_0^\infty \eta^{\xi+q}e^{-\eta^2+\frac{\sqrt{2}\eta\mu}{\sigma}}d\eta}_{I_1} \\ &\quad - \underbrace{\int_0^\infty \eta^{\xi+q}e^{-\eta^2-\frac{\sqrt{2}\eta\mu}{\sigma}}d\eta}_{I_2}\Bigg]. \quad (15)\end{aligned}$$

Solving the integral terms I_1 and I_2 with the aid of [32, eq.(20)]

$$\int_0^\infty \eta^\nu e^{-\eta^2-\eta\gamma}d\eta = 2^{-(\nu+1)/2}\Gamma(\nu+1)e^{\gamma^2/8}D_{-\nu-1}\Big(\frac{\gamma}{\sqrt{2}}\Big),$$

where

$$D_\theta(z) \triangleq 2^{\theta/2}e^{-z^2/4}\Big[\frac{\sqrt{\pi}}{\Gamma(\frac{1-\theta}{2})}\Phi\Big(-\frac{\theta}{2}, \frac{1}{2}; \frac{z^2}{2}\Big) - \frac{\sqrt{2\pi}z}{\Gamma(-\frac{\theta}{2})}\Phi\Big(\frac{1-\theta}{2}, \frac{3}{2}; \frac{z^2}{2}\Big)\Big].$$

Then, after a lengthy mathematical manipulations, we attain the desired expression for $\mathbb{E}[\eta^q|\eta|^\xi]$.

Case 2: For a nonnegative even integer q, referring to the fact that $\mathbb{E}\left[\eta^q|\eta|^\xi\right] = \mathbb{E}\left[|\eta|^{\xi+q}\right]$, we have [32]

$$\mathbb{E}\left[\eta^q|\eta|^\xi\right] = \mathbb{E}\left[|\eta|^{\xi+q}\right] = \sigma^{\xi+q}2^{\frac{\xi+q}{2}}\frac{\Gamma(\frac{\xi+q+1}{2})}{\sqrt{\pi}} \times \Phi\Big(-\frac{\xi+q}{2}, \frac{1}{2}; -\frac{\mu^2}{2\sigma^2}\Big). \quad (16)$$

To this end, we complete the proof of Proposition 1. ■

A. PERFORMANCE OF T_G

Based on the assumption that the noise variances are equal, we will derive the distributions of the GRWCD statistic under the null and alternate hypotheses in the following.

Lemma 1: For sufficiently large K and M, the distribution of the test statistic T_G under the hypothesis $\mathcal{H}_0$ can be approximated as follows:

$$T_G|\mathcal{H}_0 \sim \mathcal{N}\left(0, \sigma_0^2\right), \quad (17)$$

where σ_0^2 is given by

$$\begin{aligned}\sigma_0^2 &= \frac{1}{2}M(M-1)b_5 + \frac{2}{3}M(M-1)(M-2)b_4b_1 \\ &\quad + \frac{1}{4}M(M-1)(M-2)(M-3)b_3b_1^2 \\ &\quad + \frac{1}{3}M(M-1)(M-2)b_3b_2, \quad (18)\end{aligned}$$

in which $b_1 = \sqrt{\frac{1}{\pi K^p}}\Gamma(\frac{p+1}{2})$, $b_2 = \sqrt{\frac{1}{\pi K^{2p}}}\Gamma(\frac{2p+1}{2})$, $b_3 = \frac{1}{2K}$, $b_4 = \sqrt{\frac{1}{\pi K^{p+2}}}\Gamma(\frac{p+3}{2})$ and $b_5 = \sqrt{\frac{1}{\pi K^{2p+2}}}\Gamma(\frac{2p+3}{2})$.

Proof: For convenience of analysis, we let $\mathcal{T}_l = w_l \sum_{|n-m|=l}|a'_{mn}|^p$. Accordingly, the test statistic T_G can be rewritten as $T_G = \sum_{l=1}^{M-1}\mathcal{T}_l$. Because the random variables $\{a'_{mn}, m < n\} \sim \mathcal{N}\left(0, \frac{1}{2K}\right)$ under hypothesis $\mathcal{H}_0$ are independent [31]. Consequently, $\{\mathcal{T}_l, l = 1, \ldots, M-1\}$ are also independent. Therefore, we have $\mathbb{E}[T_G|\mathcal{H}_0] = \sum_{l=1}^{M-1}\mathbb{E}[\mathcal{T}_l|\mathcal{H}_0]$ and $\mathbb{D}[T_G|\mathcal{H}_0] = \sum_{l=1}^{M-1}\mathbb{D}[\mathcal{T}_l|\mathcal{H}_0]$. With the Proposition 1, we can derive the expectations of $\mathcal{T}_l$ and $\mathcal{T}_l^2$ as follow:

$$\begin{aligned}\mathbb{E}[\mathcal{T}_l|\mathcal{H}_0] &= \mathbb{E}\left[\left(w_l\sum_{|n-m|=l}|a'_{mn}|^p\right)\right] \\ &= \mathbb{E}\left[\sum_{|n-m|=l}a'_{mn}\left(\sum_{|n-m|=l}|a'_{mn}|^p\right)\right] \\ &= 0 \quad (19)\end{aligned}$$

and

$$\begin{aligned}\mathbb{E}\left[\mathcal{T}_l^2|\mathcal{H}_0\right] &= \mathbb{E}\left[w_l^2\left(\sum_{n-m=l}|a'_{mn}|^p\right)^2\right] \\ &= \mathbb{E}\left[\left(\sum_{n-m=l}a'_{mn}\right)^2\left(\sum_{n-m=l}|a'_{mn}|^p\right)^2\right] \\ &= \mathbb{E}\left[\sum_{n-m=l}{a'_{mn}}^2\left(\sum_{n-m=l}|a'_{mn}|^p\right)^2\right] \\ &= (M-l)\mathbb{E}\left[{a'_{mn}}^2\left(\sum_{n-m=l}|a'_{mn}|^p\right)^2\right]. \quad (20)\end{aligned}$$

Combing (19) and (20) yields

$$\begin{aligned}\mathbb{D}[\mathcal{T}_l|\mathcal{H}_0] = (M-l)\times[&b_5+2(M-l-1)b_4b_1\\&+(M-l-1)(M-l-2)b_3b_1^2\\&+(M-l-1)b_3b_2],\end{aligned}\tag{21}$$

where $b_1=\sqrt{\frac{1}{\pi K^p}}\Gamma(\frac{p+1}{2})$, $b_2=\sqrt{\frac{1}{\pi K^{2p}}}\Gamma(\frac{2p+1}{2})$, $b_3=\frac{1}{2K}$, $b_4=\sqrt{\frac{1}{\pi K^{p+2}}}\Gamma(\frac{p+3}{2})$ and $b_5=\sqrt{\frac{1}{\pi K^{2p+2}}}\Gamma(\frac{2p+3}{2})$.

As a consequence, the variance of $T_G|\mathcal{H}_0$ is given by

$$\begin{aligned}\sigma_0^2 &= \sum_{l=1}^{M-1}\mathbb{D}[\mathcal{T}_l|\mathcal{H}_0]\\&=\frac{1}{2}M(M-1)b_5+\frac{2}{3}M(M-1)(M-2)b_4b_1\\&\quad+\frac{1}{4}M(M-1)(M-2)(M-3)b_3b_1^2\\&\quad+\frac{1}{3}M(M-1)(M-2)b_3b_2.\end{aligned}\tag{22}$$

Thus, the proof is complete. ■

With a given false alarm probability P_f, the decision threshold λ_G can be theoretically calculated by

$$\lambda_G=\sigma_0 Q^{-1}\left(P_f\right),\tag{23}$$

in which $\sigma_0=\sqrt{\sigma_0^2}$ denotes the standard deviation, $Q^{-1}(\cdot)$ is the inverse function of $Q(\cdot)$ and

$$Q(x)=\frac{1}{\sqrt{2\pi}}\int_x^{\infty}e^{-t^2/2}dt.\tag{24}$$

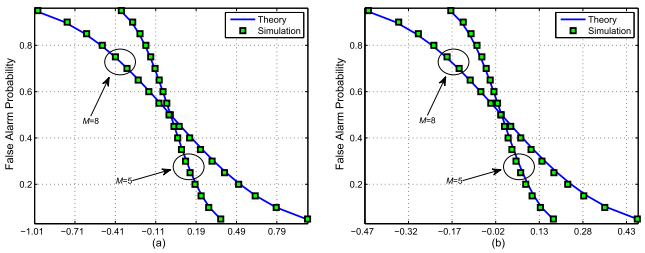

FIGURE 1. Theoretical decision threshold versus simulated decision threshold for the proposed GRWCD method, where $K=200$ and $M=\{5,8\}$ (a) $p=1/4$; (b) $p=1/2$.

In Fig. 1, we compare the theoretical decision threshold derived in (23) with the simulated decision threshold. It can be seen from Fig. 1 that the theoretical results track simulated results quite well, which confirms our analysis.

Detection Probability: In general, it is difficult to derive an accurate expression for the detection probability under the hypothesis $\mathcal{H}_1$ since the random variables

$$\{a'_{mn}, m<n\}\sim\mathcal{N}\left(\frac{\rho^{n-m}}{1+\frac{1}{\mathrm{SNR}}},\frac{1}{2K}\right)\tag{25}$$

are no longer independent [31]. Howbeit these random variables $\{a'_{mn}, m<n\}$ under at low SNR are approximately independent. By applying the central limit theorem, we have the following lemma 2.

Lemma 2: Under the hypothesis $\mathcal{H}_1$, with sufficiently large K and M, the statistic T_G at low SNR regime approximately follows the Gaussian distribution, i.e.,

$$T_G|\mathcal{H}_1\sim\mathcal{N}\left(\mu_{T_G|\mathcal{H}_1},\sigma^2_{T_G|\mathcal{H}_1}\right),\tag{26}$$

where

$$\mu_{T_G|\mathcal{H}_1}=\mathbb{E}[T_G|\mathcal{H}_1]=\sum_{l=1}^{M-1}\mathbb{E}[\mathcal{T}_l|\mathcal{H}_1],\tag{27}$$

$$\sigma^2_{T_G|\mathcal{H}_1}=\mathbb{D}[T_G|\mathcal{H}_1]=\sum_{l=1}^{M-1}\mathbb{D}[\mathcal{T}_l|\mathcal{H}_1],\tag{28}$$

in which $\mathcal{T}_l|\mathcal{H}_1=w_l\sum\limits_{n-m=l}|a'_{mn}|^p$ and

$$\begin{aligned}&\mathbb{E}[\mathcal{T}_l|\mathcal{H}_1]\\&=(M-l)\Bigg(\mu_l\sigma_1^p2^{\frac{-p}{2}}e^{-\frac{\mu_l^2}{2\sigma_1^2}}\frac{\Gamma(p+2)}{\Gamma(\frac{p+2}{2})}\Phi\Big(\frac{p+3}{2},\frac{3}{2};\frac{\mu_l^2}{2\sigma_1^2}\Big)\\&\quad+(M-l-1)\mu_l\sigma_1^p2^{\frac{p}{2}}\frac{\Gamma(\frac{p+1}{2})}{\sqrt{\pi}}\Phi\Big(-\frac{p}{2},\frac{1}{2};-\frac{\mu_l^2}{2\sigma_1^2}\Big)\Bigg)\end{aligned}$$

with $\mu_l=\frac{\rho^{n-m}}{1+\frac{1}{\mathrm{SNR}}}$ and $\sigma_1=\sqrt{\frac{1}{2K}}$. Moreover,

$$\begin{aligned}&\mathbb{D}[\mathcal{T}_l|\mathcal{H}_1]\\&=(M-l)\times\Big(g_{l1}+(M-l-1)(g_{l2}+2g_{l3}+2g_{l4}\\&\quad+2g_{l5})+(M-l-1)(M-l-2)(g_{l6}+g_{l7}\\&\quad+4g_{l8})+(M-l-1)(M-l-2)(M-l-3)g_{l9}\Big)\\&\quad-\mathbb{E}^2[\mathcal{T}_l|\mathcal{H}_1],\end{aligned}$$

where

$$g_{l1}=\sigma_1^{2p+2}2^{\frac{2p+2}{2}}\frac{\Gamma(\frac{2p+3}{2})}{\sqrt{\pi}}\Phi\Big(-\frac{2p+2}{2},\frac{1}{2};-\frac{\mu_l^2}{2\sigma_1^2}\Big),$$

$$g_{l2}=(\mu_l^2+\sigma_1^2)\left(\sigma_1^{2p}2^{\frac{2p}{2}}\frac{\Gamma(\frac{2p+1}{2})}{\sqrt{\pi}}\Phi\Big(-\frac{2p}{2},\frac{1}{2};-\frac{\mu_l^2}{2\sigma_1^2}\Big)\right),$$

$$g_{l3}=\left(\mu_l\sigma_1^p2^{\frac{-p}{2}}e^{-\frac{\mu_l^2}{2\sigma_1^2}}\frac{\Gamma(p+2)}{\Gamma(\frac{p+2}{2})}\Phi\Big(\frac{p+3}{2},\frac{3}{2};\frac{\mu_l^2}{2\sigma_1^2}\Big)\right)^2,$$

$$\begin{aligned}g_{l4}=\sigma_1^{2p+2}2^{\frac{2p+2}{2}}\frac{\Gamma(\frac{p+3}{2})}{\sqrt{\pi}}\Phi\Big(-\frac{p+2}{2},\frac{1}{2};-\frac{\mu_l^2}{2\sigma_1^2}\Big)\\\times\frac{\Gamma(\frac{p+1}{2})}{\sqrt{\pi}}\Phi\Big(-\frac{p}{2},\frac{1}{2};-\frac{\mu_l^2}{2\sigma_1^2}\Big),\end{aligned}$$

$$g_{l5}=\mu_l^2\sigma_1^{2p}2^{-p}e^{-\frac{\mu_l^2}{2\sigma_1^2}}\frac{\Gamma(2p+2)}{\Gamma(\frac{2p+2}{2})}\Phi\Big(\frac{2p+3}{2},\frac{3}{2};\frac{\mu_l^2}{2\sigma_1^2}\Big),$$

$$g_{l6}=(\mu_l^2+\sigma_1^2)\left(\sigma_1^p2^{\frac{p}{2}}\frac{\Gamma(\frac{p+1}{2})}{\sqrt{\pi}}\Phi\Big(-\frac{p}{2},\frac{1}{2};-\frac{\mu_l^2}{2\sigma_1^2}\Big)\right)^2,$$

$$g_{l7}=\mu_l^2\sigma_1^{2p}2^p\frac{\Gamma(\frac{2p+1}{2})}{\sqrt{\pi}}\Phi\Big(-p,\frac{1}{2};-\frac{\mu_l^2}{2\sigma_1^2}\Big),$$

$$g_{I8} = \mu_l^2 \sigma_1^{2p} e^{-\frac{\mu_l^2}{2\sigma_1^2}} \frac{\Gamma(p+2)}{\Gamma(\frac{p+2}{2})} \Phi\Big(\frac{p+3}{2}, \frac{3}{2}; \frac{\mu_l^2}{2\sigma_1^2}\Big) \times \frac{\Gamma(\frac{p+1}{2})}{\sqrt{\pi}} \Phi\Big(-\frac{p}{2}, \frac{1}{2}; -\frac{\mu_l^2}{2\sigma_1^2}\Big),$$

$$g_{I9} = \mu_l^2 \left(\sigma_1^p 2^{\frac{p}{2}} \frac{\Gamma(\frac{p+1}{2})}{\sqrt{\pi}} \Phi\Big(-\frac{p}{2}, \frac{1}{2}; -\frac{\mu_l^2}{2\sigma_1^2}\Big)\right)^2.$$

Proof: See Appendix. ■

Then, based on (26), the detection probability P_d for the proposed GRWCD method is obtained as

$$P_d = Q\left(\frac{\lambda_G - \mu_{T_G|\mathcal{H}_1}}{\sigma_{T_G|\mathcal{H}_1}}\right). \tag{29}$$

B. PERFORMANCE OF T_M

Based on the assumption that the noises at all antennas have different variances, the goal of this subsection is to derive the distribution of the test statistic $T_M|\mathcal{H}_0$, as given by the following Lemma 3.

Lemma 3: For sufficiently large K and M, the distribution of the test statistic T_M under the hypothesis $\mathcal{H}_0$ can be approximated as follows:

$$T_M|\mathcal{H}_0 \sim \mathcal{N}\left(0, \sigma_0^2\right), \tag{30}$$

where σ_0^2 is defined in (18).

Proof: Under the assumption of unequal per-antenna noise variances, we let $r_m^r(k)$ and $r_n^r(k)$ denote the mth and nth element of the received signal vector $\mathbf{r}^r(k)$, respectively. Conditioned on $\mathcal{H}_0$, $\{r_m^r(k) = w_m^r(k)\} \sim \mathcal{N}(0, \frac{\sigma_{wm}^2}{2})$ and $\{r_n^r(k) = w_n^r(k)\} \sim \mathcal{N}(0, \frac{\sigma_{wn}^2}{2})$. Consequently, we have

$$\mathbb{E}\left[w_m^r(k) w_n^r(k)\right] = \frac{\sigma_{wm}^2}{2}\delta(m-n) \tag{31}$$

and

$$\begin{aligned}&\mathbb{E}\left[w_m^r(k) w_n^r(k) w_{m'}^r(k) w_{n'}^r(k)\right] \\ &= \mathbb{E}\left[w_m^r(k) w_n^r(k)\right]\mathbb{E}\left[w_{m'}^r(k) w_{n'}^r(k)\right] + \mathbb{E}\left[w_m^r(k) w_{m'}^r(k)\right] \\ &\quad \times \mathbb{E}\left[w_n^r(k) w_{n'}^r(k)\right] + \mathbb{E}\left[w_m^r(k) w_{n'}^r(k)\right]\mathbb{E}\left[w_{m'}^r(k) w_n^r(k)\right]\end{aligned}$$

After some manipulations, we obtain

$$\begin{aligned}&\mathbb{E}\left[w_m^r(k) w_n^r(k) w_{m'}^r(k) w_{n'}^r(k)\right] \\ &= \begin{cases} 3\left(\frac{\sigma_{wm}^2}{2}\right)^2, & n = n' = m' = m; \\ \frac{\sigma_{wm}^2 \sigma_{wn}^2}{4}, & (m = m') \neq (n = n'); \\ 0, & \text{others.} \end{cases}\end{aligned} \tag{32}$$

As a result, for $m \neq n$, we obtain

$$\mathbb{E}\left[r_m^r(k) r_n^r(k)\right] = \frac{\sigma_{wm}^2}{2}\delta(m-n), \tag{33}$$

$$\mathbb{D}[r_m^r(k) r_n^r(k)] = \frac{\sigma_{wm}^2 \sigma_{wn}^2}{4}. \tag{34}$$

Similarly, we also have

$$\mathbb{E}\left[r_m^i(k) r_n^i(k)\right] = \frac{\sigma_{wm}^2}{2}\delta(m-n), \tag{35}$$

$$\mathbb{D}[r_m^i(k) r_n^i(k)] = \frac{\sigma_{wm}^2 \sigma_{wn}^2}{4}. \tag{36}$$

Hence, for $m \neq n$, according to central limit theorem (CLT), we have

$$\begin{aligned}\hat{a}_{mn} &= \frac{1}{2K}\sum_{k=1}^{K}\left[r_m^r(k) r_n^r(k) + r_m^i(k) r_n^i(k)\right] \\ &\sim \mathcal{N}\left(0, \frac{\frac{\sigma_{wm}^2 \sigma_{wn}^2}{4}}{2K}\right)\end{aligned} \tag{37}$$

Then,[1] we have

$$c'_{mn} \sim \mathcal{N}\left(0, \frac{1}{2K}\right), \quad m \neq n. \tag{38}$$

It can be found that, when the number of samples K is large enough, the random variables $\{a'_{mn}, m < n\}$ and $\{c'_{mn}, m < n\}$ under hypothesis $\mathcal{H}_0$ have the same distribution $\mathcal{N}\left(0, \frac{1}{2K}\right)$. Therefore, the rest of the proof is the same as that in Lemma 1. Consequently, for sufficiently large K and M, we have $T_M|\mathcal{H}_0 \sim \mathcal{N}\left(0, \sigma_0^2\right)$. ■

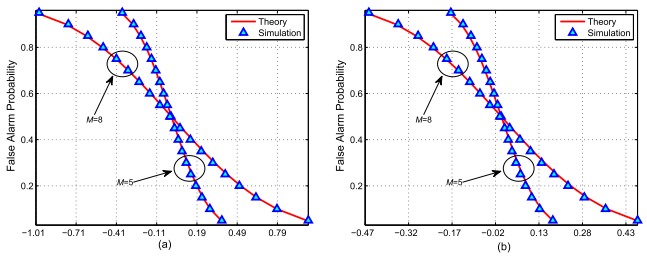

FIGURE 2. Theoretical decision threshold versus simulated decision threshold for the proposed MGRWCD method, where $K = 200$ and $M = \{5, 8\}$ (a) $p = 1/4$; (b) $p = 1/2$.

As a result, the decision threshold λ_M of the MGRWCD method can be calculated by using (23). In Fig. 2, we depict the theoretical decision threshold versus simulated decision threshold for the proposed MGRWCD method, where the noise variances are set as [0 −1 1.2 −0.8 0.6]dB for the case of $M = 5$, while the noise variances are set as [−1 0 1.5 −0.5 −1.8 1 −0.6 1.4]dB for the case of $M = 8$. It can be clearly seen that the simulated thresholds match well with theoretical results, thus validating our analysis.

V. NUMERICAL RESULTS

With the aforementioned mathematical derivations and theoretical analysis, we present experimental results to evaluate the detection performance of the proposed GRWCD and MGRWCD methods in this section.

[1] It is readily to verify that, $\{\hat{\sigma}_{wm}^2/\sigma_{wm}^2\}_{m=1}^M \sim \mathcal{N}\left(1, \frac{1}{K}\right)$, where σ_{wm}^2 denotes the true noise power at the mth antenna. When $K \to \infty$, σ_{wm}^2 can be approximately replaced by $\hat{\sigma}_{wm}^2$.

A. THE PERFORMANCE OF GRWCD METHOD

Fig. 3(a)-(d) show the theoretical (green "o" points) and simulated (solid line) receiver operating characteristic (ROC) curves of "$p = 1/4$, $M = 5$", "$p = 1/4$, $M = 8$", "$p = 1/2$, $M = 5$" and "$p = 1/2$, $M = 8$" settings, respectively, in which $\rho = 0.5$, $K = 400$ and SNR $= \{-17, -15, -13, -11\}$dB. From Fig. 3, we can see that the results obtained by Monte Carlo simulations are quite tight with the theoretical ones in the low SNR regime, validating the theoretical analysis that has been derived in (29).

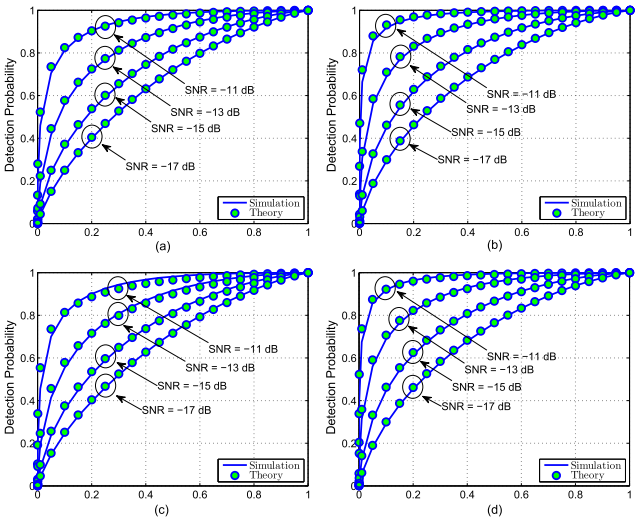

FIGURE 3. Theoretical ROC versus MC ROC, where $K = 400$ and SNR $= \{-17, -15, -13, -11\}$dB: (a) $p = 1/4$, $M = 5$; (b) $p = 1/4$, $M = 8$; (c) $p = 1/2$, $M = 5$; (d) $p = 1/2$, $M = 8$.

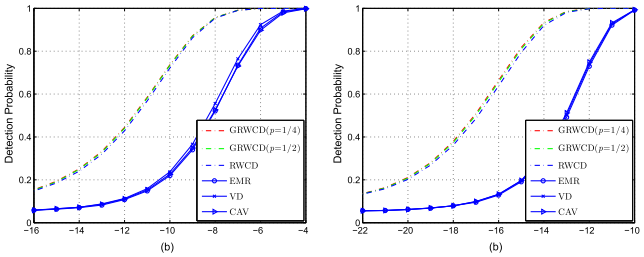

FIGURE 4. P_d versus SNR at $P_f = 0.05$, where $K = 500$: (a) $\rho = 0.4$, $M = 5$; (b) $\rho = 0.8$, $M = 7$.

Performance Comparisons: Now, we perform numerical simulations to compare the performance of the following five methods: our proposed GRWCD with $p = \{1/4, 1/2\}$, RWCD, EMR, VD and CAV. Considering the comparison fairness, the decision thresholds and false alarm probabilities of all the considered methods are obtained by simulation, each result is obtained by averaging over 10^5 Monte Carlo runs. Fig. 4 shows the detection probability P_d against SNR for all compared methods, under "$\rho = 0.4$, $M = 5$" and "$\rho = 0.8$, $M = 7$", respectively. The following observations can be made: 1) The proposed GRWCD method deliver the best performance among these compared methods in all scenarios. 2) The detection probabilities of all

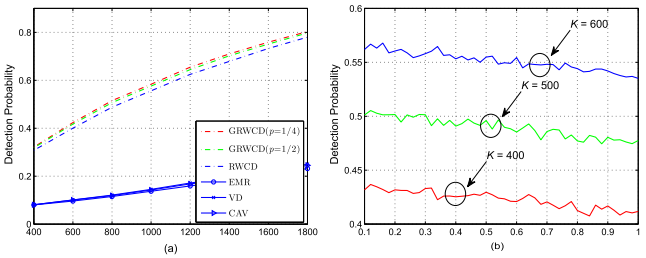

FIGURE 5. (a) P_d versus K at SNR $= -15$ dB, where $M = 5$, $\rho = 0.6$ and $P_f = 0.05$; (b) P_d versus p at SNR $= -14$ dB, where $M = 5$, $K = \{400, 500, 600\}$, $\rho = 0.6$ and $P_f = 0.05$.

the considered methods increase as the SNR increases. This is because the power of $\mathbf{h}(k)s(k)$ increases when SNR is increased, leading to substantial performance improvement. 3) By comparing Figs. 4(a) and 4(b), we can notice that the performance of all methods are improved by increasing the correlation parameter ρ. This is because all methods utilize the correlation between receive antennas to distinguish the primary signal from noise, consequently, the increase of ρ brings performance improvements to all considered methods. To further illustrate the performance of the proposed method, Fig.5 (a) depicts the detection probabilities of all compared methods with respect to the number of samples K, where $M = 5$, $P_f = 0.05$, $\rho = 0.6$, SNR $= -15$ dB and K varies from 400 to 1800. Notice from Fig. 5 (a) that, the performance of all methods improves as K increases, and our proposed method offer the best performance among all. In particular, the proposed method always outperforms the RWCD method. The reason may be that, in the low SNR regime, a power operation p $(0 < p \leq 1)$ can understate the signal component in the received samples when the PU is present.

The impact of the power operation p on the behavior of the proposed detector is shown in Fig. 5 (b), where $P_{fa} = 0.05$, $M = 5$, $K = \{400, 500, 600\}$, $\rho = 0.6$, SNR $= -14$ dB, and p varies from 0.1 to 1. As we can see that, in general, the performance of the proposed method degrades as p increases.

B. THE PERFORMANCE OF MGRWCD METHOD

In this subsection, we compare the proposed MGRWCD method with the CAV method [22], the LMPIT method [25], the Hadamard method [26], the VD method [28], and the RWCD method [31] in terms of the detection probability.

Figs. 6(a)-6(d) depict the detection probability P_d versus SNR for all compared methods with $P_f = 0.05$, where the noise variances are $[0\ -1\ 1.2\ -0.8\ 0.6]$dB and $[-1\ 0\ 1.5\ -0.5\ -1.8\ 1\ -0.6\ 1.4]$dB in Figs. 6(a)-6(b) and Figs. 6(c)-6(d), respectively. As expected, the MGRWCD method significantly outperforms the RWCD method. The reason is that the RWCD method is derived under the assumption of uniform noise variances across the antennas. Thus its performance can degrade under such non-uniform noise conditions. Moreover, our method, MGRWCD, significantly outperforms the other methods.

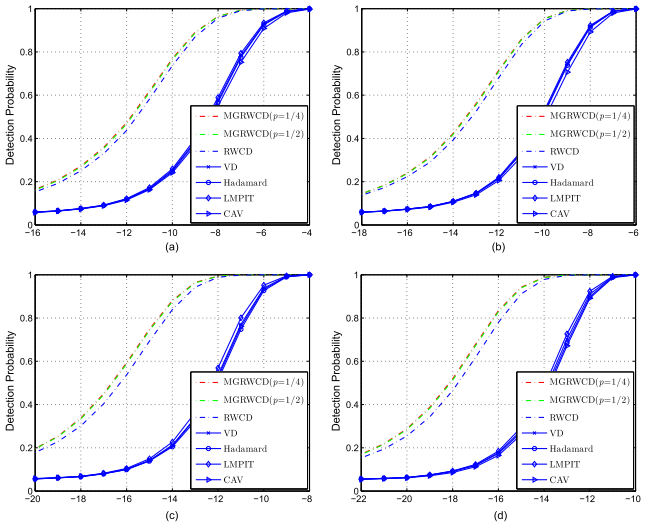

FIGURE 6. P_d versus SNR at $P_f = 0.05$, where: (a) $\rho = 0.5$, $M = 5$ and $K = 300$; (b) $\rho = 0.5$, $M = 5$ and $K = 600$; (c) $\rho = 0.8$, $M = 8$ and $K = 300$; (d) $\rho = 0.8$, $M = 8$ and $K = 600$.

VI. CONCLUSION

In this work, by adding a power operation p on the RWCD method, we develop two generalized real-valued weighted-covariance-based detection (GRWCD) methods for cognitive radio network with correlated receiving multiple antennas. In addition, we also derive the theoretical expression of the decision threshold for the proposed two methods, and the accuracy of the derived results are supported by simulations. Numerical results reveal that the proposed two methods can attain performance improvement compared with several advanced methods in the literature.

APPENDIX
PROOF OF THE LEMMA 2

Following a similar derivation procedure given in [31], we derive the expectation of $\mathcal{T}_l^2|\mathcal{H}_1$ as follows.

$$\begin{aligned}\mathbb{E}\left[\mathcal{T}_l^2|\mathcal{H}_1\right] &= \mathbb{E}\left[\left(\sum_{n-m=l} a'_{mn}\right)^2\left(\sum_{n-m=l}|a'_{mn}|^p\right)^2\right]\\ &= \mathbb{E}\Bigg[\sum_{n_1-m_1=l} a'_{m_1n_1}\sum_{n_2-m_2=l} a'_{m_2n_2}\\ &\quad\times\sum_{n_3-m_3=l}|a'_{m_3n_3}|^p\sum_{n_4-m_4=l}|a'_{m_4n_4}|^p\Bigg]. \quad (39)\end{aligned}$$

Notice that the expression of

$$\sum_{n_1-m_1=l} a'_{m_1n_1}\sum_{n_2-m_2=l} a'_{m_2n_2}\sum_{n_3-m_3=l}|a'_{m_3n_3}|^p\sum_{n_4-m_4=l}|a'_{m_4n_4}|^p$$

includes $(M-l)^4$ elements, each of them is the product of four random variables, and these elements can be divided into nine different groups according to their statistical expectations. As proved in [31], $\{a'_{mn}, m-n=l\} \sim \mathcal{N}\left(\frac{\rho^l}{1+\frac{1}{\mathrm{SNR}}}, \frac{1}{2K}\right)$. Thus, we have $\{a'_{m_1n_1}, a'_{m_2n_2}, a'_{m_3n_3}, a'_{m_4n_4}\} \sim \mathcal{N}\left(\frac{\rho^l}{1+\frac{1}{\mathrm{SNR}}}, \frac{1}{2K}\right)$. For notational convenience, we let $\mu_l = \frac{\rho^l}{1+\frac{1}{\mathrm{SNR}}}$ and $\sigma_1 = \sqrt{\frac{1}{2K}}$ in the following.

The first group comprised of $M-l$ elements, and the four random variables meet

$$a'_{m_1n_1} = a'_{m_2n_2} = a'_{m_3n_3} = a'_{m_4n_4}. \quad (40)$$

By setting $q = 2$ and $\xi = 2p$ in the Proposition 1, we obtain

$$\begin{aligned}g_{l1} &= \mathbb{E}\left[(a'_{m_1n_1})^2|a'_{m_1n_1}|^{2p}\right]\\ &= \sigma_1^{2p+2}2^{\frac{2p+2}{2}}\frac{\Gamma(\frac{2p+3}{2})}{\sqrt{\pi}}\Phi\Big(-\frac{2p+2}{2},\frac{1}{2};-\frac{\mu_l^2}{2\sigma_1^2}\Big).\end{aligned}$$

The second group comprised of $(M-l)(M-l-l)$ elements, and the four random variables meet

$$\left(a'_{m_1n_1} = a'_{m_2n_2}\right) \neq \left(a'_{m_3n_3} = a'_{m_4n_4}\right). \quad (41)$$

By setting $q = 0, \xi = 2p$ in the Proposition 1, and using the fact that $\mathbb{E}\left[(a'_{m_1n_1})^2\right] = \mu_l^2 + \sigma_1^2$, we have

$$\begin{aligned}g_{l2} &= \mathbb{E}\left[(a'_{m_1n_1})^2|a'_{m_3n_3}|^{2p}\right]\\ &= \mathbb{E}\left[(a'_{m_1n_1})^2\right]\mathbb{E}\left[|a'_{m_3n_3}|^{2p}\right]\\ &= (\mu_l^2+\sigma_1^2)\times\left(\sigma_1^{2p}2^{\frac{2p}{2}}\frac{\Gamma(\frac{2p+1}{2})}{\sqrt{\pi}}\Phi\Big(-\frac{2p}{2},\frac{1}{2};-\frac{\mu_l^2}{2\sigma_1^2}\Big)\right)\\ &= (\mu_l^2+\sigma_1^2)\left(\sigma_1^{2p}2^{\frac{2p}{2}}\frac{\Gamma(\frac{2p+1}{2})}{\sqrt{\pi}}\Phi\Big(-\frac{2p}{2},\frac{1}{2};-\frac{\mu_l^2}{2\sigma_1^2}\Big)\right).\end{aligned}$$

The third group comprised of $2(M-l)(M-l-l)$ elements, and the four random variables meet

$$\left(a'_{m_1n_1} = a'_{m_3n_3}\right) \neq \left(a'_{m_2n_2} = a'_{m_4n_4}\right); \quad (42)$$

or

$$\left(a'_{m_1n_1} = a'_{m_4n_4}\right) \neq \left(a'_{m_2n_2} = a'_{m_3n_3}\right). \quad (43)$$

Then, by setting $q = 1$ and $\xi = p$ in the Proposition 1, we get

$$\begin{aligned}g_{l3} &= \mathbb{E}\left[(a'_{m_1n_1})a'_{m_2n_2}|a'_{m_3n_3}|^p|a'_{m_4n_4}|^p\right]\\ &= \mathbb{E}^2\left[a'_{m_1n_1}|a'_{m_1n_1}|^p\right]\\ &= \left(\mu_l\sigma_1^p2^{\frac{-p}{2}}e^{-\frac{\mu_l^2}{2\sigma_1^2}}\frac{\Gamma(p+2)}{\Gamma(\frac{p+2}{2})}\Phi\Big(\frac{p+3}{2},\frac{3}{2};\frac{\mu_l^2}{2\sigma_1^2}\Big)\right)^2.\end{aligned}$$

The fourth group comprised of $2(M-l)(M-l-l)$ elements, and the four random variables meet

$$\left(a'_{m_1n_1} = a'_{m_2n_2} = a'_{m_3n_3}\right) \neq \left(a'_{m_4n_4}\right); \quad (44)$$

or

$$\left(a'_{m_1n_1} = a'_{m_2n_2} = a'_{m_4n_4}\right) \neq \left(a'_{m_3n_3}\right). \quad (45)$$

Then, letting $q=0,\xi=p+2$ and $q=0,\xi=p$ in the Proposition 1, respectively, we have

$$\begin{aligned}g_{l4}&=\mathbb{E}\left[(a'_{m_1n_1})a'_{m_2n_2}|a'_{m_3n_3}|^p|a'_{m_4n_4}|^p\right]\\&=\mathbb{E}\left[(a'_{m_1n_1})^2|a'_{m_1n_1}|^p\right]\mathbb{E}\left[|a'_{m_3n_3}|^p\right]\\&=\mathbb{E}\left[|a'_{m_1n_1}|^{p+2}\right]\mathbb{E}\left[|a'_{m_3n_3}|^p\right]\\&=\left(\sigma_1^{p+2}2^{\frac{p+2}{2}}\frac{\Gamma(\frac{p+3}{2})}{\sqrt{\pi}}\Phi\Big(-\frac{p+2}{2},\frac{1}{2};-\frac{\mu_l^2}{2\sigma_1^2}\Big)\right)\\&\quad\times\left(\sigma_1^p2^{\frac{p}{2}}\frac{\Gamma(\frac{p+1}{2})}{\sqrt{\pi}}\Phi\Big(-\frac{p}{2},\frac{1}{2};-\frac{\mu_l^2}{2\sigma_1^2}\Big)\right)\\&=\sigma_1^{2p+2}2^{\frac{2p+2}{2}}\frac{\Gamma(\frac{p+3}{2})}{\sqrt{\pi}}\Phi\Big(-\frac{p+2}{2},\frac{1}{2};-\frac{\mu_l^2}{2\sigma_1^2}\Big)\\&\quad\times\frac{\Gamma(\frac{p+1}{2})}{\sqrt{\pi}}\Phi\Big(-\frac{p}{2},\frac{1}{2};-\frac{\mu_l^2}{2\sigma_1^2}\Big).\end{aligned}$$

The fifth group comprised of $2(M-l)(M-l-l)$ elements, and the four random variables

$$\left(a'_{m_1n_1}=a'_{m_3n_3}=a'_{m_4n_4}\right)\neq\left(a'_{m_2n_2}\right);\tag{46}$$

or

$$\left(a'_{m_1n_1}\right)\neq\left(a'_{m_2n_2}=a'_{m_3n_3}=a'_{m_4n_4}\right).\tag{47}$$

Then, by setting $q=1$ and $\xi=2p$ in the Proposition 1, and using the fact that $\mathbb{E}\left[a'_{m_2n_2}\right]=\mu_l$, we have

$$\begin{aligned}g_{l5}&=\mathbb{E}\left[a'_{m_1n_1}a'_{m_2n_2}|a'_{m_3n_3}|^p|a'_{m_4n_4}|^p\right]\\&=\mathbb{E}\left[a'_{m_1n_1}|a'_{m_1n_1}|^{2p}\right]\mathbb{E}\left[a'_{m_2n_2}\right]\\&=\mu_l\sigma_1^{2p}2^{\frac{-2p}{2}}e^{-\frac{\mu_l^2}{2\sigma_1^2}}\frac{\Gamma(2p+2)}{\Gamma(\frac{2p+2}{2})}\Phi\Big(\frac{2p+3}{2},\frac{3}{2};\frac{\mu_l^2}{2\sigma_1^2}\Big)\times\mu_l\\&=\mu_l^2\sigma_1^{2p}2^{-p}e^{-\frac{\mu_l^2}{2\sigma_1^2}}\frac{\Gamma(2p+2)}{\Gamma(\frac{2p+2}{2})}\Phi\Big(\frac{2p+3}{2},\frac{3}{2};\frac{\mu_l^2}{2\sigma_1^2}\Big).\end{aligned}$$

The sixth group comprised of$(M-l)(M-l-l)(M-l-2)$ elements, and the four random variables meet

$$\left(a'_{m_1n_1}=a'_{m_2n_2}\right)\neq a'_{m_3n_3}\neq a'_{m_4n_4}.\tag{48}$$

Using the fact that $\mathbb{E}\left[(a'_{m_1n_1})^2\right]=\mu_l^2+\sigma_1^2$ and letting $q=0$ and $\xi=p$ in the Proposition 1, we have

$$\begin{aligned}g_{l6}&=\mathbb{E}\left[a'_{m_1n_1}a'_{m_2n_2}|a'_{m_3n_3}|^p|a'_{m_4n_4}|^p\right]\\&=\mathbb{E}\left[(a'_{m_1n_1})^2\right]\mathbb{E}\left[|a'_{m_3n_3}|^p\right]\mathbb{E}\left[|a'_{m_4n_4}|^p\right]\\&=\mathbb{E}\left[(a'_{m_1n_1})^2\right]\mathbb{E}^2\left[|a'_{m_3n_3}|^p\right]\\&=(\mu_l^2+\sigma_1^2)\times\left(\sigma_1^p2^{\frac{p}{2}}\frac{\Gamma(\frac{p+1}{2})}{\sqrt{\pi}}\Phi\Big(-\frac{p}{2},\frac{1}{2};-\frac{\mu_l^2}{2\sigma_1^2}\Big)\right)^2\\&=(\mu_l^2+\sigma_1^2)\left(\sigma_1^p2^{\frac{p}{2}}\frac{\Gamma(\frac{p+1}{2})}{\sqrt{\pi}}\Phi\Big(-\frac{p}{2},\frac{1}{2};-\frac{\mu_l^2}{2\sigma_1^2}\Big)\right)^2.\end{aligned}$$

The seventh group comprised of $(M-l)(M-l-l)(M-l-2)$ elements, and the four random variables meet

$$a'_{m_1n_1}\neq a'_{m_2n_2}\neq\left(a'_{m_3n_3}=a'_{m_4n_4}\right).\tag{49}$$

Then, by setting $q=0,\xi=2p$ in the Proposition 1, and using the fact that $\mathbb{E}^2\left[(a'_{m_1n_1})\right]=\mu_l^2$, we have

$$\begin{aligned}g_{l7}&=\mathbb{E}\left[a'_{m_1n_1}a'_{m_2n_2}|a'_{m_3n_3}|^p|a'_{m_4n_4}|^p\right]\\&=\mathbb{E}^2\left[(a'_{m_1n_1})\right]\mathbb{E}\left[|a'_{m_3n_3}|^{2p}\right]\\&=\mu_l^2\times\sigma_1^{2p}2^{\frac{2p}{2}}\frac{\Gamma(\frac{2p+1}{2})}{\sqrt{\pi}}\Phi\Big(-\frac{2p}{2},\frac{1}{2};-\frac{\mu_l^2}{2\sigma_1^2}\Big)\\&=\mu_l^2\sigma_1^{2p}2^p\frac{\Gamma(\frac{2p+1}{2})}{\sqrt{\pi}}\Phi\Big(-p,\frac{1}{2};-\frac{\mu_l^2}{2\sigma_1^2}\Big).\end{aligned}$$

The eighth group comprised of $4(M-l)(M-l-l)(M-l-2)$ elements, and the four random variables meet

$$\begin{aligned}\left(a'_{m_1n_1}=a'_{m_3n_3}\right)&\neq a'_{m_2n_2}\neq a'_{m_4n_4};\\\left(a'_{m_1n_1}=a'_{m_4n_4}\right)&\neq a'_{m_2n_2}\neq a'_{m_3n_3};\\a'_{m_1n_1}&\neq\left(a'_{m_2n_2}=a'_{m_3n_3}\right)\neq a'_{m_4n_4};\end{aligned}\tag{50}$$

or

$$a'_{m_1n_1}\neq\left(a'_{m_2n_2}=a'_{m_4n_4}\right)\neq a'_{m_3n_3}.\tag{51}$$

Then, by setting $q=1,\xi=p$ and $q=0,\xi=p$ in the Proposition 1, respectively, and using the fact that $\mathbb{E}\left[a'_{m_2n_2}\right]=\mu_l$, we have

$$\begin{aligned}g_{l8}&=\mathbb{E}\left[a'_{m_1n_1}a'_{m_2n_2}|a'_{m_3n_3}|^p|a'_{m_4n_4}|^p\right]\\&=\mathbb{E}\left[a'_{m_1n_1}|a'_{m_1n_1}|^p\right]\mathbb{E}\left[a'_{m_2n_2}\right]\mathbb{E}\left[|a'_{m_4n_4}|^p\right]\\&=\mu_l\sigma_1^p2^{\frac{-p}{2}}e^{-\frac{\mu_l^2}{2\sigma_1^2}}\frac{\Gamma(p+2)}{\Gamma(\frac{p+2}{2})}\Phi\Big(\frac{p+3}{2},\frac{3}{2};\frac{\mu_l^2}{2\sigma_1^2}\Big)\times\mu_l\\&\quad\times\sigma_1^p2^{\frac{p}{2}}\frac{\Gamma(\frac{p+1}{2})}{\sqrt{\pi}}\Phi\Big(-\frac{p}{2},\frac{1}{2};-\frac{\mu^2}{2\sigma_1^2}\Big)\\&=\mu_l^2\sigma_1^{2p}e^{-\frac{\mu_l^2}{2\sigma_1^2}}\frac{\Gamma(p+2)}{\Gamma(\frac{p+2}{2})}\Phi\Big(\frac{p+3}{2},\frac{3}{2};\frac{\mu_l^2}{2\sigma_1^2}\Big)\\&\quad\times\frac{\Gamma(\frac{p+1}{2})}{\sqrt{\pi}}\Phi\Big(-\frac{p}{2},\frac{1}{2};-\frac{\mu_l^2}{2\sigma_1^2}\Big).\end{aligned}$$

The ninth group comprised of $(M-l)(M-l-l)(M-l-2)(M-l-3)$ elements, and the four random variables meet

$$a'_{m_1n_1}\neq a'_{m_2n_2}\neq a'_{m_3n_3}\neq a'_{m_4n_4}.\tag{52}$$

Using the fact that $\mathbb{E}\left[a'_{m_1n_1}\right]=\mu_l$ and $\mathbb{E}\left[a'_{m_2n_2}\right]=\mu_l$, while letting $q=0,\xi=p$ in the Proposition 1, we have

$$\begin{aligned}g_{l9}&=\mathbb{E}\left[a'_{m_1n_1}a'_{m_2n_2}|a'_{m_3n_3}|^p|a'_{m_4n_4}|^p\right]\\&=\mathbb{E}\left[(a'_{m_1n_1})\right]\mathbb{E}\left[(a'_{m_2n_2})\right]\mathbb{E}\left[|a'_{m_3n_3}|^p\right]\mathbb{E}\left[|a'_{m_4n_4}|^p\right]\\&=\mathbb{E}^2\left[(a'_{m_1n_1})\right]\mathbb{E}^2\left[|a'_{m_3n_3}|^p\right]\\&=\mu_l^2\left(\sigma_1^p2^{\frac{p}{2}}\frac{\Gamma(\frac{p+1}{2})}{\sqrt{\pi}}\Phi\Big(-\frac{p}{2},\frac{1}{2};-\frac{\mu_l^2}{2\sigma_1^2}\Big)\right)^2.\end{aligned}$$

Thus, the variance of $\mathcal{T}_l$ under $\mathcal{H}_1$ is derived as

$$\begin{aligned}\mathbb{D}[\mathcal{T}_l|\mathcal{H}_1]&=(M-l)\\&\quad\times\Big(g_{l1}+(M-l-1)(g_{l2}+2g_{l3}+2g_{l4}+2g_{l5})\\&\quad+(M-l-1)(M-l-2)(g_{l6}+g_{l7}+4g_{l8})\\&\quad+(M-l-1)(M-l-2)(M-l-3)g_{l9}\Big)\\&\quad-\mathbb{E}^2[\mathcal{T}_l|\mathcal{H}_1].\end{aligned}\tag{53}$$

REFERENCES

[1] X. Hong, J. Wang, C.-X. Wang, and J. Shi, "Cognitive radio in 5G: A perspective on energy-spectral efficiency trade-off," *IEEE Commun. Mag.*, vol. 52, no. 7, pp. 46–53, Jul. 2014.
[2] M. Agiwal, A. Roy, and N. Saxena, "Next generation 5G wireless networks: A comprehensive survey," *IEEE Commun. Surveys Tut.*, vol. 18, no. 3, pp. 1617–1655, 3rd Quart., 2016.
[3] I. Kakalou, K. E. Psannis, P. Krawiec, and R. Badea, "Cognitive radio network and network service chaining toward 5G: Challenges and requirements," *IEEE Commun. Mag.*, vol. 55, no. 11, pp. 145–151, Nov. 2017.
[4] H. Ding *et al.*, "Cognitive capacity harvesting networks: Architectural evolution toward future cognitive radio networks," *IEEE Commun. Surveys Tuts.*, vol. 19, no. 3, pp. 1902–1923, 3rd Quart., 2017.
[5] T. Yucek and H. Arslan, "A survey of spectrum sensing algorithms for cognitive radio applications," *IEEE Commun. Surveys Tuts.*, vol. 11, no. 1, pp. 116–130, 1st Quart., 2009.
[6] E. Axell, G. Leus, E. G. Larsson, and H. V. Poor, "Spectrum sensing for cognitive radio: State-of-the-art and recent advances," *IEEE Signal Process. Mag.*, vol. 29, no. 3, pp. 101–116, May 2012.
[7] A. Ali and W. Hamouda, "Advances on spectrum sensing for cognitive radio networks: Theory and applications," *IEEE Commun. Surveys Tuts.*, vol. 19, no. 2, pp. 1277–1304, 2nd Quart., 2016.
[8] F. F. Digham, M.-S. Alouini, and M. K. Simon, "On the energy detection of unknown signals over fading channels," *IEEE Trans. Commun.*, vol. 55, no. 1, pp. 21–24, Jan. 2007.
[9] Y. Chen, "Improved energy detector for random signals in Gaussian noise," *IEEE Trans. Wireless Commun.*, vol. 9, no. 2, pp. 558–563, Feb. 2010.
[10] S. Atapattu, C. Tellambura, and H. Jiang, "Energy detection based cooperative spectrum sensing in cognitive radio networks," *IEEE Trans. Wireless Commun.*, vol. 10, no. 4, pp. 1232–1241, Apr. 2011.
[11] L. Gahane, P. K. Sharma, N. Varshney, T. A. Tsiftsis, and P. Kumar, "An improved energy detector for mobile cognitive users over generalized fading channels," *IEEE Trans. Commun.*, vol. 66, no. 2, pp. 534–545, Feb. 2018.
[12] V. Kostylev and I. Gres, "Characteristics of p-norm signal detection in gaussian mixture noise," *IEEE Trans. Veh. Technol.*, vol. 67, no. 4, pp. 2973–2981, Apr. 2018.
[13] H. V. Poor, *An Introduction to Signal Detection and Estimation*. New York, NY, USA: Springer-Verlag, 1994.
[14] S. M. Kay, *Fundamentals of Statistical Signal Processing, Volume II: Detection Theory*. Upper Saddle River, NJ, USA: Prentice-Hall, 1998.
[15] H.-S. Chen, W. Gao, and D. G. Daut, "Signature based spectrum sensing algorithms for IEEE 802.22 WRAN," in *Proc. IEEE Int. Conf. Commun. (ICC)*. Glasgow, U.K., Jun. 2007, pp. 6487–6492.
[16] A. V. Dandawate and G. B. Giannakis, "Statistical tests for presence of cyclostationarity," *IEEE Trans. Signal Process.*, vol. 42, no. 9, pp. 2355–2369, Sep. 1994.
[17] J. Lunden, V. Koivunen, A. Huttunen, and H. V. Poor, "Collaborative cyclostationary spectrum sensing for cognitive radio systems," *IEEE Trans. Signal Process.*, vol. 57, no. 11, pp. 4182–4195, Nov. 2009.
[18] J. Lunden, S. A. Kassam, and V. Koivunen, "Robust nonparametric cyclic correlation-based spectrum sensing for cognitive radio," *IEEE Trans. Signal Process.*, vol. 58, no. 1, pp. 38–52, Jan. 2010.
[19] A. Tani and R. Fantacci, "A low-complexity cyclostationary-based spectrum sensing for UWB and WiMAX coexistence with noise uncertainty," *IEEE Trans. Veh. Technol.*, vol. 59, no. 6, pp. 2940–2950, Jul. 2010.
[20] R. Tandra and A. Sahai, "SNR walls for signal detection," *IEEE J. Sel. Topics Signal Process.*, vol. 2, no. 1, pp. 4–17, Feb. 2008.
[21] Y. Zeng and Y.-C. Liang, "Eigenvalue-based spectrum sensing algorithms for cognitive radio," *IEEE Trans. Commun.*, vol. 57, no. 6, pp. 1784–1793, Jun. 2009.
[22] Y. Zeng and Y.-C. Liang, "Spectrum-sensing algorithms for cognitive radio based on statistical covariances," *IEEE Trans. Veh. Technol.*, vol. 58, no. 4, pp. 1804–1815, May 2009.
[23] R. Zhang, T. J. Lim, Y.-C. Liang, and Y. Zeng, "Multi-antenna based spectrum sensing for cognitive radios: A GLRT approach," *IEEE Trans. Commun.*, vol. 58, no. 1, pp. 84–88, Jan. 2010.
[24] A. Taherpour, M. Nasiri-Kenari, and S. Gazor, "Multiple antenna spectrum sensing in cognitive radios," *IEEE Trans. Wireless Commun.*, vol. 9, no. 2, pp. 814–823, Feb. 2010.
[25] D. Ramirez, J. Via, and I. Santamaria, "The locally most powerful test for multiantenna spectrum sensing with uncalibrated receivers," in *Proc. IEEE Int. Conf. Acoust., Speech Signal Process. (ICASSP)*, Mar. 2012, pp. 3437–3440.
[26] L. Huang, Y. Xiao, H. C. So, and J. Fang, "Accurate performance analysis of Hadamard ratio test for robust spectrum sensing," *IEEE Trans. Wireless Commun.*, vol. 14, no. 2, pp. 750–758, Feb. 2015.
[27] L. Huang, H.-C. So, and C. Qian, "Volume-based method for spectrum sensing," *Digit. Signal Process.*, vol. 28, pp. 48–56, May 2014.
[28] L. Huang, C. Qian, Y. Xiao, and Q. T. Zhang, "Performance analysis of volume-based spectrum sensing for cognitive radio," *IEEE Trans. Wireless Commun.*, vol. 14, no. 1, pp. 317–330, Jan. 2015.
[29] L. Huang, J. Fang, K. Liu, H. C. So, and H. Li, "An eigenvalue-moment-ratio approach to blind spectrum sensing for cognitive radio under sample-starving environment," *IEEE Trans. Veh. Technol.*, vol. 64, no. 8, pp. 3465–3480, Aug. 2015.
[30] M. Jin, Q. Guo, J. Xi, Y. Li, Y. Yu, and D. D. Huang, "Spectrum sensing using weighted covariance matrix in Rayleigh fading channels," *IEEE Trans. Veh. Technol.*, vol. 64, no. 11, pp. 5137–5148, Nov. 2015.
[31] A.-Z. Chen and Z.-P. Shi, "A real-valued weighted covariance-based detection method for cognitive radio networks with correlated multiple antennas," *IEEE Commun. Lett.*, vol. 22, no. 11, pp. 2290–2293, Nov. 2018.
[32] A. Winkelbauer. (2012). "Moments and absolute moments of the normal distribution." [Online]. Available: https://arxiv.org/abs/1209.4340
[33] A. Nafkha and B. Aziz, "Closed-form approximation for the performance of finite sample-based energy detection using correlated receiving antennas," *IEEE Wireless Commun. Lett.*, vol. 3, no. 6, pp. 577–580, Dec. 2014.

AN-ZHI CHEN is currently pursuing the Ph.D. degree with the National Key Laboratory of Communications, University of Electronic Science and Technology of China (UESTC), Chengdu, China. His current research interests include cognitive radio, statistical signal processing, and signal detection.

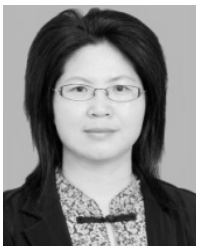

ZHI-PING SHI received the M.Sc. and Ph.D. degrees from Southwest Jiaotong University, Chengdu, China, in 1998 and 2005, respectively. She has two years of postdoctoral experience with the University of Electronic Science and Technology of China (UESTC), from 2005 to 2007. In 2007, she joined the School of Communication and Information, UESTC, where she is currently a Professor with the National Key Laboratory of Science and Technology on Communications. She spent one year as a Visiting Scholar with Lehigh University, Bethlehem, PA, USA, from 2009 to 2010. Her research interests include coding theory, cognitive radio, and wireless communication.

JIAN XIONG received the B.Sc. and M.Sc. degrees from the University of Electronic Science and Technology of China, Chengdu, China, in 1999 and 2002, respectively, and the Ph.D. degree from Shanghai Jiao Tong University (SJTU), Shanghai, China, in 2006. He was a Visiting Scholar with Columbia University, in 2015. He is currently an Associate Professor with the Image Communication and Networking Engineering Institute, SJTU. He has published over 40 journal or conference papers. He holds over 40 patents, including 25 awarded patents. His current research interests include wireless wideband transmission technologies, networking, and caching technologies of converged wideband and broadcast systems. He was a recipient of one Best Journal Paper Award (IEEE TB'14) and three Conference Best Paper Awards (IEEE/BMSB'16, IEEE/SSC'16, and IEEE/BMSB'18). He has been the TPC Co-Chair of the IEEE International Symposium on Broadband Multimedia Systems and Broadcasting, since 2010.